Pergamon

Int. J. Heat Mass Transfer. Vol. 37, Suppl. 1, pp. 3–8, 1994

0017–9310/94 $6.00 + 0.00

0017–9310(93)E0065–O

Transition from transpiration to film cooling†

E. R. G. ECKERT and H. H. CHO

Heat Transfer Laboratory, Mechanical Engineering Department, University of Minnesota, Minneapolis, MN 55455, U.S.A.

Abstract—Heat transfer characteristics of transpiration cooling devices encompass Stanton numbers and the temperature increase in the transpired wall. These were calculated for ideal transpiration cooling and for transpiration cooling of a permeable or perforated wall with a turbulent boundary layer covering its surface and compared with experimental results for full coverage film cooling.

INTRODUCTION

EARLY studies on transpiration and film cooling were published in the 1950s by Hartnett and Eckert [1, 2]. Film cooling has since found wide acceptance in various applications, especially in gas turbines. Transpiration cooling offers the promise of higher effectiveness but has not been used extensively as yet. The present paper compares the thermal performance of the two methods and studies the transition from total coverage film cooling to transpiration cooling.

IDEAL TRANSPIRATION COOLING

Transpiration cooling is used to protect a solid wall from the detrimental effect of a hot fluid, usually a hot gas. The wall consists of a porous material and a coolant is moving through the pores creating a cool layer on the hot gas side of the wall protecting it. The analysis of the transpiration cooling method in this section will be based on an idealized model which should result in a limiting value of its efficiency: the cross-sectional areas of the channels and their distances will be assumed vanishingly small so that the coolant seeps with a locally uniform velocity v_w through the wall. In addition, it is stipulated that both fluids have the same properties (density ρ, specific heat c_p, thermal conductivity k), that the fluids can be considered incompressible and that the velocities are small so that frictional heating can be neglected. In the numerical computations, the fluid in the mainstream and the coolant are postulated to be air ($Pr = 0.7$). The hot fluid moves with a constant velocity, u_s, along the wall forming a turbulent boundary layer. Figure 1 sketches this situation. The main stream has a temperature T_s, the wall surface and the coolant leaving this surface have the temperature T_w. The conductive heat flux q_w at the wall surface is obtained by a solution of the time averaged Navier–Stokes equations with the boundary conditions;

at the surface ($y = 0$): $u = 0$, $v = v_w$, $T = T_w$.

Relations describing the turbulent character of the flow are required for the solution of the Navier–Stokes equation. The two-parameter κ–ε relations and empirical correlations for the near wall region are used, the equations are solved on a high speed computer with the SIMPLER algorithm (Patankar [3]). The turbulent parameters κ–ε are predicted by a revised form of the Low-Reynolds-Number κ–ε model (Cho and Goldstein [4]).

The heat flux q_w transported from the hot fluid into the wall by conduction is obtained from the solution of the Navier–Stokes equations with the relation

$$q_w = -k\left(\frac{\partial T}{\partial y}\right)_w \tag{1}$$

and a Stanton number as a dimensionless expression of the heat transfer process is defined as

$$St_w = \frac{q_w}{\rho c_p u_s (T_s - T_w)}. \tag{2}$$

Dimensional analysis predicts that the Stanton number St_w is a function of the blowing rate

$$M = \frac{v_w}{u_s} \tag{3}$$

the mainstream Reynolds number

$$Re_x = \frac{u_s x}{\nu} \tag{4}$$

and the Prandtl number.

Figures 2–4 present the results of the described analysis and compare these with data found in the literature. For the analysis it was postulated that the porous wall is preceded by a solid section on which a hydrodynamic and a thermal boundary layer have developed. The porous section begins at a mainstream Reynolds number $Re_x \approx 2 \times 10^5$. The solid wall has the same temperature as the porous section.

In Fig. 2(a), the ratio of the Stanton number St_w to the Stanton number St_0 for turbulent convection on a solid wall is plotted over the ratio M/St_0. The fact

† Dedicated to J. P. Hartnett on his seventieth birthday.

NOMENCLATURE

c_p	specific heat
d	channel width
K	acceleration parameter
k	thermal conductivity
L	wall thickness
l	mixing length
M	blowing rate
Pr	Prandtl number
q	heat flux
Re	Reynolds number
s	distance between channels
St	Stanton number
T	temperature
u, v	velocity components
x, y	coordinates.

Greek symbols

$\delta_{0.99}$	boundary layer thickness
ν	kinematic viscosity
ρ	density
τ_w	wall shear stress.

Subscripts

a	air
c	coolant
d	refers to channel width
o	without transpiration
s	mainstream
sw	solid matrix
w	wall
x	in x direction.

that the calculated data points do not quite line up on a curve indicates a slight effect of the Reynolds number Re_x. The two curves denoted 1 and 2 refer to Fig. 2(b) in which experimental values obtained by various investigations are plotted in the same way as in Fig. 2(a). The two curves 1 and 2 present empirical correlations found in the literature. Figure 2(b) is reproduced from a book by Kutateladze and Leontiev [5].

Figure 3(a) lists the ratio of the turbulent mixing length l to the boundary layer thickness (based on the wall distance y at which the velocity u is 0.99 of the free stream velocity) as function of the dimensionless wall distance $y/\delta_{0.99}$. These are calculated values which can be compared with measured values in Fig. 3(b) (Kays and Moffat [6]). One recognizes that fluid injection into the boundary layer has little influence on the mixing length.

A strong influence of blowing, however, is predicted by the analysis in Fig. 4 where the dimensionless Reynolds stress—the ratio of the time mean of the product of the fluctuating velocity components u' and v' to the time mean velocity u_s squared—is listed for blowing rates from zero to 0.008. The abscissa is $y^+ = y[\sqrt{(\tau_w/\rho)}/\nu]$ with τ_w indicating the wall shear stress. It is interesting to observe that transpiration

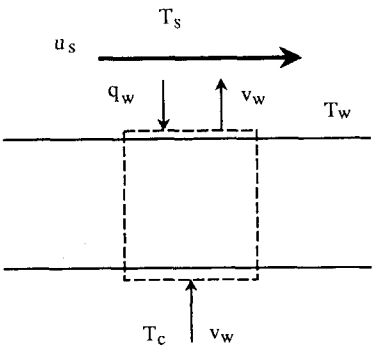

FIG. 1. Cross-section of ideal transpiration cooled wall.

alters the Reynolds stress distribution but has only a small effect on the mixing length.

The temperature T_w is not the temperature with which the coolant is admitted because continuity requires that a heat flux q_w given by equation (1) moves from the surface into the interior of the wall (Eckert and Drake [7]). It encounters there a counterflow of coolant and accordingly the temperature gradient in the porous wall decreases with increasing y. An energy balance on the control volume bordered by the surfaces sketched as dashed lines in Fig. 1 results in the equation

$$q_w = \rho c_p v_w (T_w - T_c) \tag{5}$$

with T_c denoting the coolant temperature at the place where the temperature gradient has decreased asymptotically to zero and conductive heat transfer is negligible. Sidewise energy transport is zero because the wall temperature has been stipulated locally constant. A combination of equations (2), (3) and (5) results in the dimensionless temperature ratio

$$\frac{T_w - T_c}{T_s - T_w} = \frac{St_w}{M}. \tag{6}$$

In Fig. 2, the blowing parameter and the Stanton number are of equal order of magnitude. This means that the temperature increase $T_w - T_c$ of the coolant is also of the same order of magnitude as the temperature difference in the boundary layer. Usually the hot stream temperature T_s and the wall surface temperature T_w are prescribed for the design of a transpiration cooling arrangement. The Stanton number St_w can then be calculated or obtained from tabulated experimental values. The temperature T_c at which the coolant is provided follows then from equation (6).

On the other hand it is difficult to measure the wall surface temperature exactly whereas the coolant temperature T_c can be easily measured. It is then con-

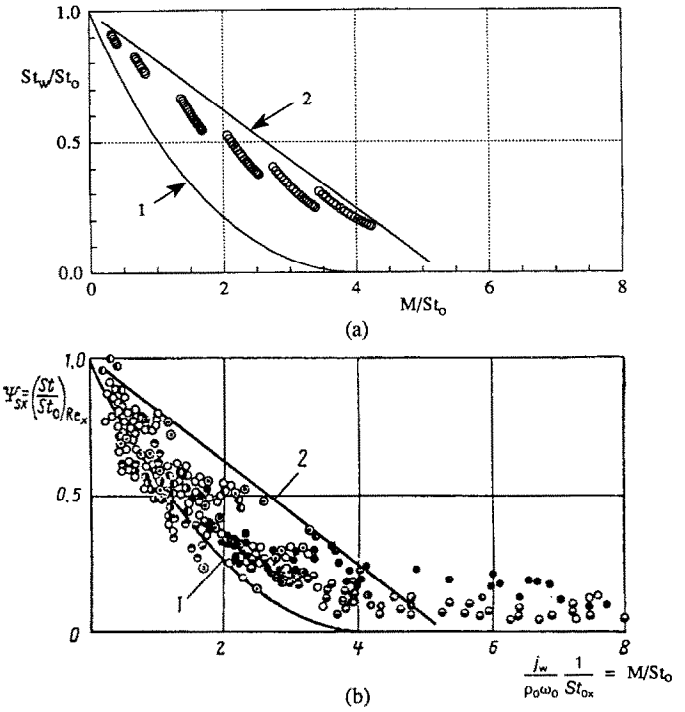

FIG. 2. Comparison of Stanton numbers calculated by present analysis (Fig. 2(a)) with those compiled by Kutateladze and Leontiev [5] (Fig. 2(b)). St_w Stanton number with transpiration, St_o without transpiration, M blowing rate.

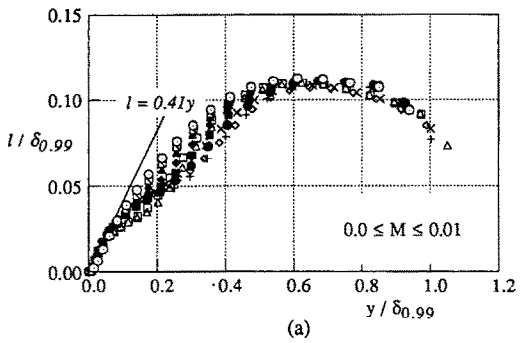

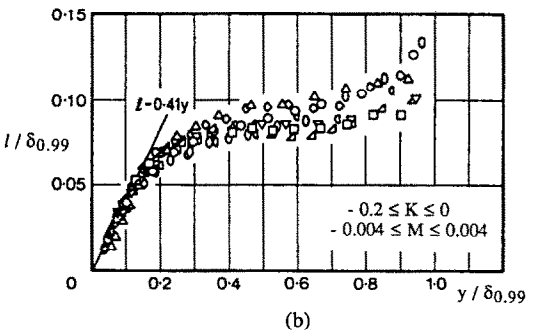

FIG. 3. Comparison of mixing lengths obtained by present analysis (Fig. 3(a)) with those measured by Kays and Moffat [6] for flow over a flat plate with deceleration (Fig. 3(b)). l mixing length, $\delta_{0.99}$ boundary layer thickness, y wall distance, M blowing rate, K acceleration parameter

venient to define a Stanton number based on the difference $T_s - T_c$ according to the equation

$$St_c = \frac{q_w}{\rho c_p u_s (T_s - T_c)}. \tag{7}$$

The following relation exists between the two Stanton numbers according to the previous equations

$$St_c = \frac{St_w}{\frac{St_w}{M} + 1}. \tag{8}$$

TRANSPIRATION COOLING WITH A PERMEABLE MATRIX

Full coverage film cooling data in the literature are for distances s of the cooling channels which are a multiple of the channel diameter d (for instance 5 or 10). One has to expect that film cooling approaches the condition of transpiration cooling as the ratios s/d approaches the value 1. This will be investigated with the use of the model sketched in Fig. 5. A solid wall has a regular pattern of slots with the width d and a distance s. The flow and temperature field are, therefore, two dimensional in their time averaged values. Approximately, this model should also describe parameters averaged in the direction normal to the plane of drawing for the arrangement of rows of cooling holes instead of slots. For the situation that $s/d = 1$,

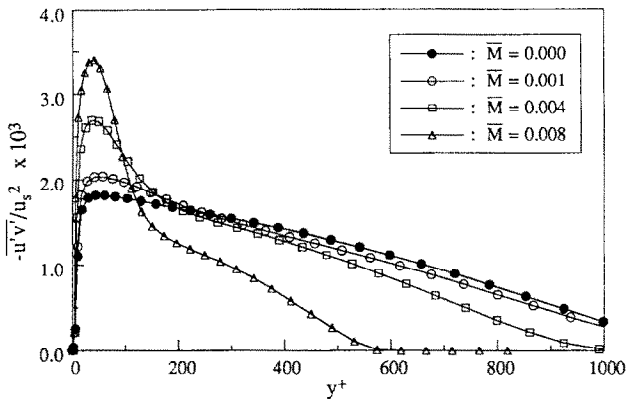

FIG. 4. Dimensionless Reynolds stress $-\overline{u'v'}/u_s^2$ without ($\bar{M} = 0$) and with ($\bar{M} = 0.001$–0.008) transpiration. y^+ dimensionless wall distance

this model is identical to the ideal transpiration cooling model.

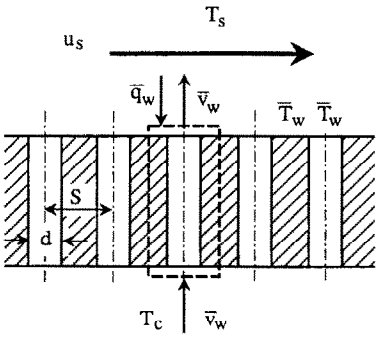

FIG. 5. Cross-section of perforated wall with transpiration cooling.

Solutions of the time averaged Navier–Stokes equations are presented in Fig. 6 for the situation that $s/d = 2$. The equations were solved with boundary conditions which may be explained with the help of Fig. 5. The velocity v_w has a prescribed value at the exit of the channels and a value zero at the solid part of the wall surface. The coolant flow out of the channels is stipulated laminar and the wall surface temperature T_w is assumed locally constant with the same value at the channel exits and the solid parts of the wall. The grid for the numerical calculation was too coarse to expect that local differences in the Stanton numbers at the hole exits and at the film cooled solid portions would be correctly depicted by the solution. Therefore, the Stanton numbers in Fig. 6 are based on heat fluxes q_w averaged over areas containing

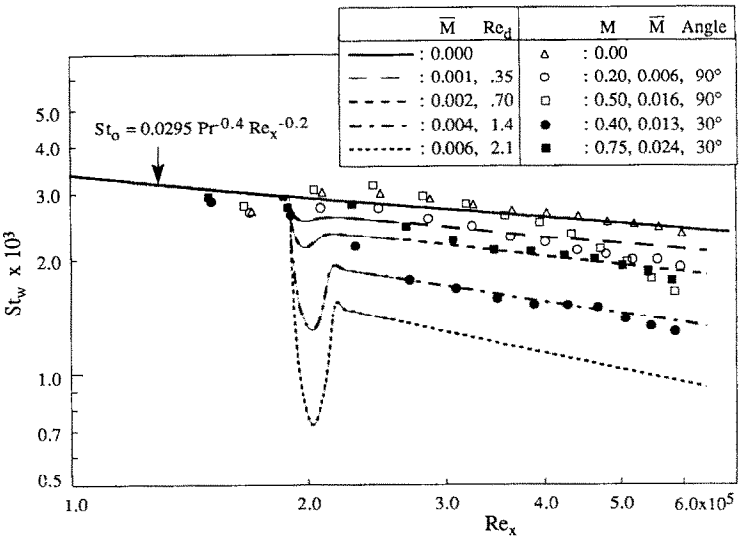

FIG. 6. Stanton number St_w for a perforated wall without transpiration cooling ($\bar{M} = 0$) and with transpiration cooling for four blowing rates ($\bar{M} = 0.001$–0.006) compared with values measured by Moffat *et al.* [9, 10] for normal and slanted injection. Re_d channel Reynolds number, $(v_w d)/\nu$.

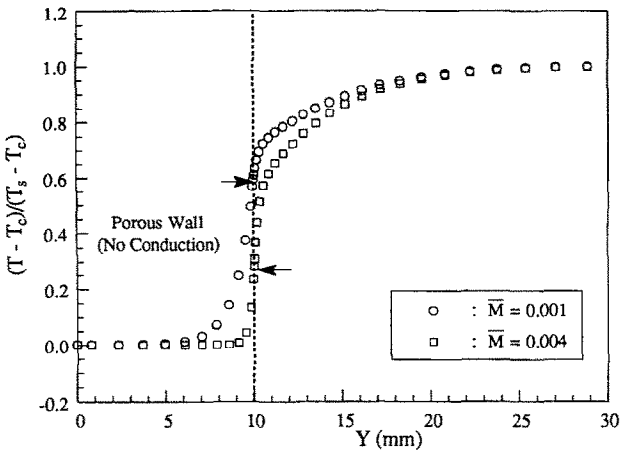

FIG. 7. Temperature variation of the coolant within the channels of the perforated wall and in the boundary layer. The wall has zero conductivity. Y distance from coolant entry side of perforated wall.

channel exits as well as solid parts. In the same way an average coolant velocity is defined as the volume flow per unit area of wall surface (containing open and solid parts) and the blowing rate is formed with this averaged velocity. Such averaged values are indicated by a bar, $\bar{v}_w$, $\bar{M}$. Otherwise equations (1)–(8) apply here also.

The porous wall is again preceded by a solid one which is cooled convectively to a temperature T_w. Hydrodynamic and thermal boundary layers develop along that part of the wall. The Stanton number St_o calculated with the program described before is plotted as the solid line. It is also described by the listed equation and is in excellent agreement with experimental results reported in the literature. Transpiration cooling starts at $Re_x \approx 2 \times 10^5$. Four curves present Stanton numbers for the averaged blowing rates $\bar{M}$ equal to 0.001–0.006. The channel size is described by a channel Reynolds number

$$Re_d = \frac{v_w d}{\nu}. \tag{9}$$

This parameter varies from 0.35 to 2.1. The length ratio d/x is equal for all Re_d values listed in the figure

$$\frac{d}{x} = \frac{Re_d}{Re_x \bar{M}}.$$

Calculations not reported here indicate that the Stanton numbers change very little with the channel Reynolds number as long as the flow at the exit of the channels remains laminar and as long as no major separation of the flow occurs (Eckert *et al.* [8]).

Also listed in the figure are Stanton numbers measured by Choe *et al.* [9] and Crawford *et al.* [10] for cylindrical channels arranged in a square pattern with a spacing to diameter ratio of 5 and with the channel axis either normal to the wall surface or inclined by 30 degrees toward the surface in the flow direction. A

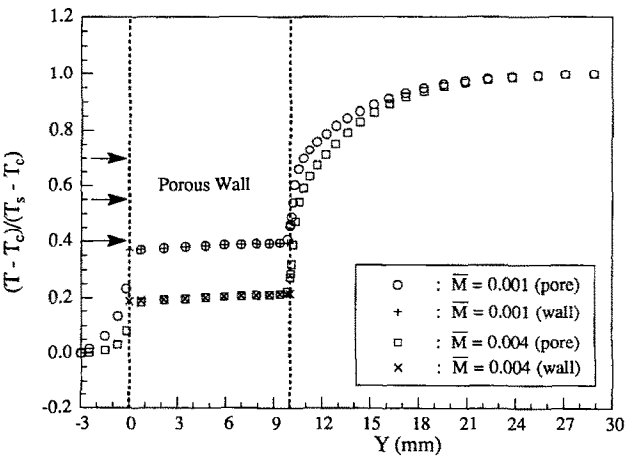

FIG. 8. Temperature variation of the coolant within the channels of the perforated wall and in the boundary layer. The conductivity of the matrix is 500 times that of the coolant. Y distance from coolant entry side of perforated wall.

comparison of the calculated values with the measured ones for inclined injection indicates that the same Stanton number can be achieved with 1/3 to 1/12 of the averaged blowing rate where the channel rows are spaced with two times the diameter and the ratio is even larger for normal injection.

The development of composite materials should be helpful for the production of walls with closely spaced passages. The pressure drop through the passages can be tailored by providing passages with curved or tortuous passages.

The difference between the wall surface temperature T_w and the coolant entry temperature T_c can again be obtained by the energy balance on the control volume with the surface shown in Fig. 5 by dashed lines. Equation (5) describes it and equation (6) determines the difference between T_w and T_c. It is remarkable that this temperature difference is the same regardless of the value of the conductivity of the solid wall matrix. The shape of the temperature field in the transpiration cooled wall, however, is influenced by the conductivity of the solid matrix. Figures 7 and 8 present it for two situations.

In Fig. 7, the temperature profile of the coolant in the porous wall and that in the boundary layer is shown for two blowing rates $\bar{M}$ in a dimensionless presentation. The two arrows indicate the wall surface temperatures T_w. Equation 6 then determines the Stanton number. The thermal conductivity of the solid matrix has for this figure the value zero. This presents, for instance, the situation in which the mass transfer analogy is used to simulate transpiration cooling.

In Fig. 8, the conductivity of the solid matrix has a value 500 times as large as that of the cooling air. This corresponds, approximately, to the conductivity of stainless steel. There are almost no temperature gradients in the porous wall and the difference between the coolant and the solid temperature is so small that it cannot be shown in the figure.

REFERENCES

1. J. P. Hartnett and E. R. G. Eckert, Mass transfer cooling in a laminar boundary layer with constant fluid properties, *Trans. Am. Soc. Mech. Engrs* **79**, 247–254 (1957).
2. J. P. Hartnett, R. C. Birkebak and E. R. G. Eckert, *International Developments in Heat Transfer*, Vol. IV, p. 682. ASME, New York (1961).
3. S. V. Patankar, *Numerical Heat Transfer and Fluid Flow*. Hemisphere McGraw-Hill, New York (1980).
4. H. H. Cho and R. J. Goldstein, An improved Low-Reynolds-Number κ–ε turbulence model for recirculating flows, *Int. J. Heat Mass Transfer* (in press).
5. S. S. Kutateladze and A. I. Leontiev, *Heat Transfer, Mass Transfer, and Friction in Turbulent Boundary Layers*, pp. 161–165. Hemisphere, New York (1990).
6. W. M. Kays and R. J. Moffat, The behaviour of transpired turbulent boundary layers. In *Studies in Convection* (Edited by B. E. Launder), Vol. 1, pp. 223–319 (1975).
7. E. R. G. Eckert and R. M. Drake, Jr., *Analysis of Heat and Mass Transfer*, pp. 445–451. McGraw-Hill, New York (1972).
8. E. R. G. Eckert, R. J. Goldstein and H. H. Cho, Heat Transfer Laboratory Report No. 107, Mechanical Engineering Dept., University of Minnesota, Minneapolis, Minnesota (1993).
9. H. Choe, W. M. Kays and R. J. Moffat, The turbulent boundary layer on a full-coverage film cooled surface : an experimental heat transfer study with normal injection, Report HMT-22, Stanford University, Department of Mechanical Engineering, Stanford, Calif. (1976).
10. M. E. Crawford, W. M. Kays and R. J. Moffat, Heat transfer to a full-coverage film-cooled surface with 30° slant-hole injection, Report HMT-25, Stanford University, Department of Mechanical Engineering, Stanford, Calif. (1976).